Sparkling feather reflections of a bird-of-paradise explained by finite-difference time-domain modeling

Bodo D. Wilts[a,1,2], Kristel Michielsen[b], Hans De Raedt[a], and Doekele G. Stavenga[a,2]

[a]Computational Physics, Zernike Institute for Advanced Materials, University of Groningen, NL-9747AG, Groningen, The Netherlands; and [b]Institute for Advanced Simulation, Jülich Supercomputing Centre, Research Centre Jülich, D-52425 Jülich, Germany

Edited by David A. Weitz, Harvard University, Cambridge, MA, and approved January 29, 2014 (received for review December 18, 2013)

Birds-of-paradise are nature's prime examples of the evolution of color by sexual selection. Their brilliant, structurally colored feathers play a principal role in mating displays. The structural coloration of both the occipital and breast feathers of the bird-of-paradise Lawes' parotia is produced by melanin rodlets arranged in layers, together acting as interference reflectors. Light reflection by the silvery colored occipital feathers is unidirectional as in a classical multilayer, but the reflection by the richly colored breast feathers is three-directional and extraordinarily complex. Here we show that the reflection properties of both feather types can be quantitatively explained by finite-difference time-domain modeling using realistic feather anatomies and experimentally determined refractive index dispersion values of keratin and melanin. The results elucidate the interplay between avian coloration and vision and indicate tuning of the mating displays to the spectral properties of the avian visual system.

biophotonics | body colors | courtship | signaling | reflectance

Birds-of-paradise are best known for their magnificent coloration. Living isolated on Papua New Guinea and its satellite islands (1), the absence of predators has allowed these birds to become extremely specialized for female sexual selection (2). Male birds-of-paradise have evolved extravagant ornamental traits, with intricate sounds and ritualized sets of dance steps and movements accompanied by simultaneous elaborate feather movements, all combined in beautiful displays to win the favor of females (1–4). Among the 39 species of birds-of-paradise almost all colors of the rainbow can be found, and often the males advertise themselves with brilliant, vivid colors framed within a jet-black background. The females on the other hand have dull brownish plumage which has remained in its ancestral color state (1, 2).

Whereas the biological purpose of the colorful displays is relatively well understood (1, 2), the coloration mechanisms of the birds' displays and the connection to the visual system of the animals are poorly explored. Feather coloration can be generally categorized in two forms: pigmentary and structural. Randomly arranged, inhomogeneous media containing pigments are colored, because the pigments absorb the diffusely scattered light in a restricted wavelength range. For instance, carotenoids cause the colorful yellow or red feathers of many songbirds (5), and the ubiquitous, broad-band absorbing pigment melanin causes feathers to be black (6). Structural colors occur in feather barbs due to quasiordered spongy structures, and in feather barbules due to melanosomes—nanosized, melanin-containing granules—regularly arranged in layers within a keratin matrix, resulting in directional reflections because of constructive interference (7–11). Differences in the morphology of the structural colored feathers, i.e., in the dimensions of the spongy structured barbs or the melanosome multilayers in the barbules, can modify the color of the reflected light and can thus tune the optical properties of the feathers. Indeed, the various bird-of-paradise feathers impressively demonstrate how modifications of morphological traits can lead to dramatic changes of visual effects.

We here investigate the occipital (nape) and breast feathers of the males of the bird-of-paradise species Lawes' parotia (Fig. 1*A*, *Parotia lawesii*, Ramsey, 1885; Aves: Passeriformes: Paradisaeidae), which seduce females with a stunning display of strongly colored feathers during an extravagant dancing ritual, the so-called "ballerina dance" (2, 3, 12, 13). The plumage of male Lawes' parotia consists of mostly jet-black feathers (Fig. 1*A*). These feathers contrast strongly with silver-colored, occipital (nape) feathers, which reflect light specularly, due to a precisely spaced, layered arrangement of melanosomes (11) in a keratin matrix (Fig. 1 *B* and *D*). The multicolored breast feathers also contain a multilayer of melanosomes, but these are much smaller and more densely packed (Fig. 1 *C* and *E*). The breast feathers' unique, boomerang-shaped cross-section, enveloped by a thin film, gives rise to three-directional reflections that allow rapid switching between an orange, green, or blue color when the bird makes its moves (3, 12).

Whereas the essential features of the occipital feather reflections are well described by classical multilayer theory (13), the optical properties of the breast feathers have not yet been quantitatively treated, because the morphology of the barbules is too complex to apply analytical models (12). To unravel the reflection properties of the morphologically complex breast feathers as determined by spectrometry and imaging scatterometry, we applied an advanced computational approach, finite-difference time-domain (FDTD) modeling. FDTD allows fully explicit computation of the interaction of light with matter by directly solving Maxwell's equations in the time domain (14–16). By using the known barbule anatomy and detailed measurements of the refractive index values of melanized feather components (13), FDTD modeling has provided detailed understanding of the silvery reflectance of the occipital feathers as well as allowed substantial, quantitative insight into the optical mechanisms underlying the

Significance

Birds-of-paradise are brilliant examples of colorful displays in nature. The dazzling colors of the display, used in ritualized dances to attract the attention of mates, arise from the interference and diffraction of light within photonic nanostructures on their feathers. This study reports a quantitative investigation of the complex photonic structures by connecting experimental photonics with a state of the art computational model. The methods used in this study may be applied to numerous applications, e.g., for optimized photonic crystal designs. Here it has allowed us to unveil the coloration mechanisms in the feathers of a bird-of-paradise and investigate the connection of feather colors to the avian visual system.

Author contributions: B.D.W. and D.G.S. designed research; B.D.W., K.M., H.D.R., and D.G.S. performed research; K.M. and H.D.R. contributed new analytic tools; B.D.W. and D.G.S. analyzed data; and B.D.W. and D.G.S. wrote the paper.

The authors declare no conflict of interest.

This article is a PNAS Direct Submission.

[1]Present address: Cavendish Laboratory, Department of Physics, University of Cambridge, Cambridge CB3 0HE, United Kingdom.

[2]To whom correspondence may be addressed. E-mail: bdw36@cam.ac.uk or D.G.Stavenga@rug.nl.

This article contains supporting information online at www.pnas.org/lookup/suppl/doi:10.1073/pnas.1323611111/-/DCSupplemental.

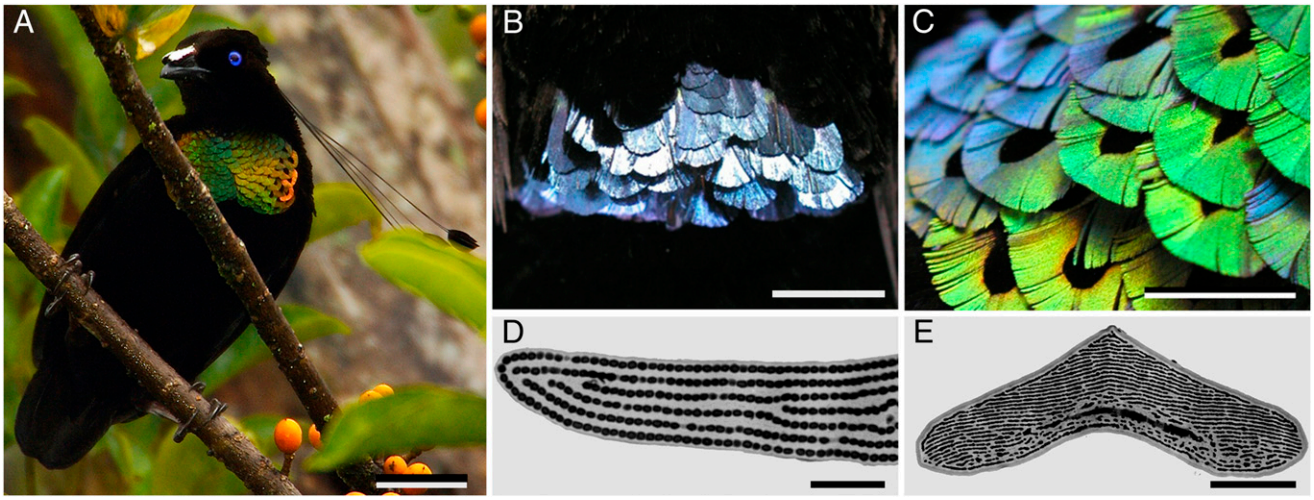

Fig. 1. Bird of paradise Lawes' parotia, *P. lawesii*. (*A*) Habitat view (photo courtesy of Tim Laman). (*B*) Photograph of the nape of the bird, showing the silver-colored, mirror-like occipital feathers. (*C*) Slightly oblique view of the breast feathers showing the drastic variation in color along the differently inclined feathers. (*D*) TEM of a barbule of an occipital feather. (*E*) TEM of a barbule of a breast feather. Scale bars: (*A*) 5 cm, (*B*) 1 cm, (*C*) 1 cm, (*D*) 2 μm, (*E*) 5 μm.

three-directional reflections of the breast feathers. The calculated reflectance spectra suggest that the reflection characteristics of the male breast feathers are tuned to the female's color vision properties.

Results

Barbule Morphology. The feather barbules of both the breast and nape area contain well-ordered layers of melanosomes surrounded by a keratin cortex (Fig. 1 *D* and *E*). Whereas the occipital feather barbules are more or less flat and contain layers of melanosomes having a diameter of ∼250 ± 20 nm with an interlayer spacing of ∼400 ± 20 nm, the melanosomes of the breast feather barbules have a much smaller diameter, ∼120 ± 15 nm, and the interlayer spacing here is ∼230 ± 20 nm. Furthermore, the layers in the breast feather barbules are not flat but skewed, resulting in a boomerang-shaped cross-section (12). The strongly different morphologies of the barbules of the breast and occipital feathers create very different spatial and spectral reflection properties as revealed by imaging scatterometry and angle-dependent reflectometry.

Angle- and Wavelength-Dependence of the Occipital Feathers' Reflectance. We investigated the barbules' spatial light-scattering pattern with an imaging scatterometer (*Methods*). Illumination of an occipital feather with the primary, narrow-aperture light beam (17) yielded a very directional reflection pattern, like that of a mirror. Rotation of the feather over angles of 10°, 20°, 30°, and 40° resulted in reflected beams directed into angles of 20°, 40°, 60°, and 80°, respectively (Fig. 2 *A* and *B*). With local illumination, the occipital feathers thus behave as a classical optical multilayer, consisting of a stack of parallel thin films.

For specular objects, hemispherical illumination, which is light incident from all angles above the object, can be applied to document the angle-dependent reflection properties in a single image. This is realized with the secondary, wide-angled (180°) beam of the scatterometer (18, 19). When illuminating the occipital feathers with unpolarized light, an increasing angle of light incidence causes a changing color of the reflected light, symmetric around the center from blue through violet to white (Fig. 2*C*). The white-colored reflectance at high angles is due to the fact that for very large angles of incidence the reflectance approaches 100%, for all wavelengths for all specular systems, including multilayer structures. Upon adding a vertically polarizing filter into the incident light beam (Fig. 2*D*; see also Movie S1), reflectance minima emerge in the vertical plane, that is, for transverse magnetic (TM)-polarized light, showing a Brewster's angle of ∼60° (20).

To be able to perform a quantitative analysis of the optical properties of the occipital feathers, we measured the feathers' reflectance as a function of illumination angle for transverse electric (TE)- as well as for TM-polarized light with a goniometric fiber setup (Fig. 2 *E* and *G*). The occipital feathers have for normal light incidence a reflectance maximum in the near-IR, at ∼1,300 nm, whereas the reflectance in the visible wavelength range slightly varies, yielding a silvery-bluish color (Figs. 1*B* and 2 *E* and *G*). The reflectance spectra measured for a number of angles of light incidence strongly depend on the polarization direction, in agreement with the scatterogram (Fig. 2*D*). With an increase in the angle of light incidence, the IR peak of the reflectance spectra shifts to shorter wavelengths. Whereas the reflectance amplitude for TE-polarized light monotonically increases with increasing angle of light incidence, the reflectance amplitude for TM-polarized light decreases up to an incident angle of ∼55–60°, but above that angle the amplitude increases again.

FDTD Modeling of the Occipital Feather Reflectance. To connect the anatomy of the feathers with the spatial and spectral measurements, we applied FDTD modeling. The anatomical cross-sections of Fig. 1 *D* was grayscaled, placed in a simulation volume, and, subsequently, complex refractive index values were assigned for different grayscale values using the previously measured refractive index dispersion of the barbules' material components (keratin and melanin; Fig. S1 and refs. 13, 21). Two-dimensional transmission electron microscopy (TEM) cross-sections were extended into a 3D simulation volume.

The angle- and polarization-dependent reflectance spectra calculated for the occipital feather (Fig. 2 *F* and *H*) are strikingly similar to the experimental spectra (Fig. 2 *E* and *G*) with respect to reflectance amplitude, peak position as well as peak width, confirming the structural basis of the color (Figs. S2 and S3).

Breast Feather Reflections. Light reflections by the breast and occipital feathers drastically differ. Local illumination of a breast feather barbule with the primary beam of the scatterometer yields a complex scattering pattern with three colored areas

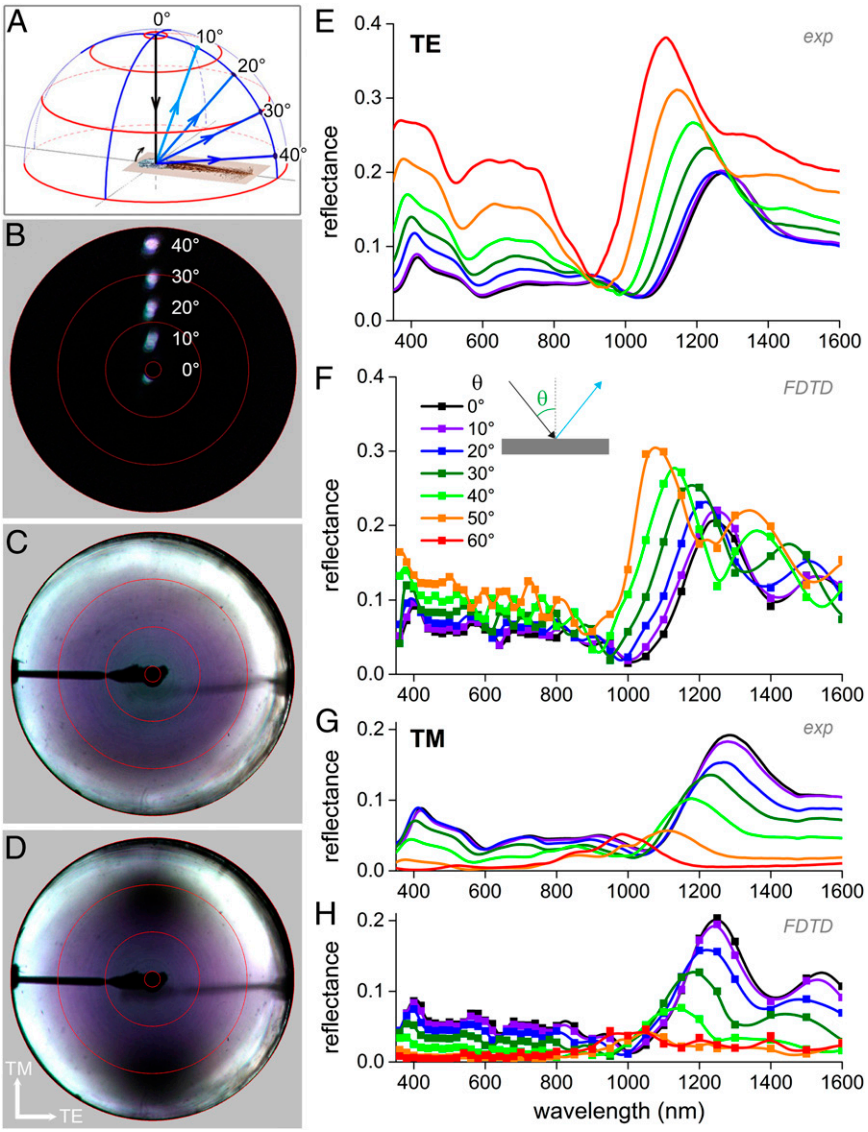

Fig. 2. Optics of the occipital feather barbules. (*A*) Diagram of light reflection by an occipital feather barbule rotated in steps of 10°, from 0°, to 10°, 20°, 30°, and 40° resulting in reflected beams into angular directions of 20°, 40°, 60°, and 80°. (*B*) Superposition of light-scattering patterns for different angles of illumination as sketched in *A*. Illumination of a barbule with a narrow-aperture (~5°) light beam yielded a similar narrow-aperture directionally reflected beam, demonstrating the specular characteristics of the occipital feather. (*C*) Light-scattering pattern of the feather oriented normal to the central axis of the imaging scatterometer and illuminated hemispherically (full aperture 180°) with unpolarized light. (*D*) As *C*, but with illumination of the barbule with TM polarized light. The reflection of TM-polarized light becomes minimal at Brewster's angle (dark spots around −60° and +60° at the vertical axis; see also Movie S1). The red circles in *B*–*D* indicate angular directions of 5°, 30°, 60°, and 90° and correspond to the red circles in *A*. (*E*) Angle-dependent reflectance spectra measured when applying TE-polarized light. (*F*) Angle-dependent reflectance spectra calculated for TE-polarized light by FDTD modeling. (*G* and *H*) As *E* and *F* for TM-polarized light.

(Fig. 3*A*): a central yellow-orange spot, resulting from the multilayer inside the barbule, flanked by two cyan-colored patches in angular directions of about 60° with respect to the central spot, resulting from the barbule envelope acting as a thin film (see ref. 12).

Hemispherical illumination is inappropriate as a research tool for the breast feather barbule, due to overlap of the reflection patterns of the three different optical components that cause the three colored areas when applying narrow-aperture illumination. The iridescence of each of the three reflection components of Fig. 3*A* can still be usefully investigated, however, by applying slit illumination, as is shown in Fig. 3*B*. We inserted a line-shaped diaphragm into the secondary illumination beam, allowing illumination with broad-angled light (180°) in the longitudinal symmetry plane of the barbule. As expected, the interference patterns of the two side beams are identical and show the typical iridescence of a thin film, characteristically shifting from blue to violet and white with increasing angle of light incidence (Fig. 3*B*). The iridescence of the central spot, however, is somewhat atypical for a layered reflector. As usual, with increasing reflection angle, the hue of the reflected light shifts toward shorter wavelengths (10, 19), but instead of increasing, the reflectance amplitude sharply falls off for increasing reflection angles and vanishes for reflection angles ≥60°. Measurement of the angle-dependent reflectance documents this even more clearly. The peak wavelength of the reflectance spectra measured in the longitudinal symmetry plane, i.e., with illumination and detection parallel to the barbules' long axis, shifts with increasing angle of

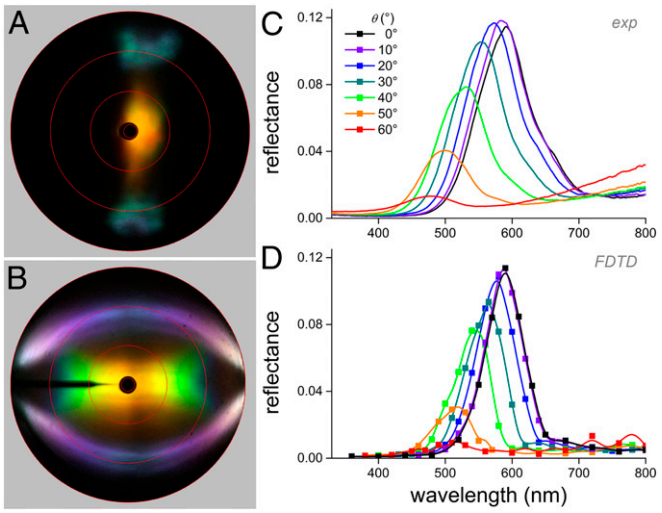

Fig. 3. Optics of the breast feather barbules. (*A*) Light-scattering pattern resulting from normal illumination of a barbule with a narrow-aperture (~5°) light beam, showing a central golden-yellow-colored spot and two cyan-colored patches, representing reflections into angular directions of about −60° and +60° from the center. (*B*) Light-scattering pattern resulting from illumination with a slit light source with a narrow aperture in the vertical direction and a 180° aperture horizontally, showing the barbule's iridescence. (*C*) Angle-dependent reflectance spectra measured with unpolarized light. (*D*) Angle-dependent reflectance spectra calculated for unpolarized light by FDTD modeling.

incidence toward shorter wavelengths whereas the amplitude strongly diminishes (Fig. 3*C*).

FDTD Modeling of the Breast Feather Reflections. The complex anatomy of the breast feather barbules does not allow analytical modeling of the spatial and spectral reflection properties. Using the same FDTD modeling procedure as for the occipital feathers, reflectance spectra very similar to the experimental spectra are simulated for the breast feather barbules (Fig. 3 *C* and *D* and Fig. S4).

FDTD modeling allows the direct visualization of light propagation in the barbules' photonic structures. Fig. 4*A* shows a superposition of the electric field intensities for normally incident light of wavelengths 420 nm (blue) and 610 nm (orange). As expected from the experimental results, the incident light beam is split up into three individual optical components: orange light is directionally reflected, due to constructive light interference in the melanin–keratin multilayer, whereas blue light is effectively reflected by the skewed thin films of the barbules, yielding two components with angular directions of ~60° (compare with Fig. 3*A*, and see time-lapse movies of Movie S2).

The light-scattering pattern resulting with narrow-aperture incident light is obtained by calculating the light distribution in the far field. Fig. 4*B* shows the superimposed light-scattering patterns calculated for a light beam delivered by a point source in the horizontal plane, the incidence angle of which was changed in steps of 10° from −60° to 60°. In the experiment of Fig. 3*B*, the illumination was not a point but a slit light source, but the experimental and simulated light-scattering patterns nevertheless correspond well. A minor difference is the color of the thin-film side reflection, which is cyan-green (Fig. 4*B*) instead of blue (Fig. 3*B*) and is presumably due to the specific barbule cross-section of Fig. 1*E* that was used in the calculations. The reflectance spectra of the side strongly depend on the thickness of the barbules cortex, which is naturally somewhat variable (compare also the color of the side reflections in Fig. 3 *A* and *B* and Fig. S5).

Considering the simulated light reflections of the breast feathers more closely reveals that the angled thin films cause the diminishing reflectance of the central multilayer structure when the angle of light incidence increases. This is due to an increased reflectance of the tilted thin films occurring with an increased angle of incidence (Fig. 4*C*). In other words, for increasing angles of light incidence, the incident light is progressively reflected at the tilted thin films, which reduces the light reaching the multilayers inside the barbule.

Biological Implications and Connection to Bird Vision. Male parotias perform a characteristic ballerina dance in a sunny lek to win the favor of females that are sitting in an elevated position on a branch above the males (Fig. 5*A* and refs. 1–3). The dance display usually consists of up to seven stages, starting with a "bow" by the male (22). During the dance, the males shape-shift: from the normal bird-like appearance they take various bizarre forms, by making use of the different functionalized feathers (see pages 126–129 of ref. 2 for different snapshots). Both the occipital and breast feathers reflect directionally and thus leave a strong visual impression on the female sitting perched above the male, especially when the bird moves quickly and the colors shift in a blink of the eye.

To get more insight into the biological significance of the display, we considered how the angle-dependent reflections stimulate the visual system, i.e., whether the reflectance spectra are tuned to the spectral sensitivities of the photoreceptors. This might reveal possible tuning and evolution of the display to the bird's color vision. The photoreceptor spectral sensitivities of bird-of-paradise are similar to those of the pigeon (2, 23). The four photoreceptors of pigeons have peak sensitivities at 404 nm (violet-sensitive), 480 nm (short-wavelength–sensitive), 547 nm

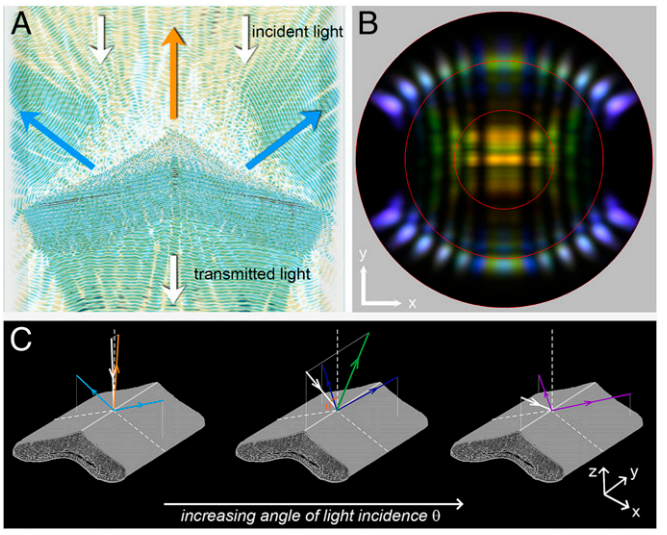

Fig. 4. FDTD modeling of the breast feather barbule. (*A*) Two superimposed video frames for normal illumination of a breast feather barbule with 420 nm (blue) and 610 nm (orange) light. The time-lapse movies for these wavelengths are shown in Movie S2. The propagation direction of the incident and transmitted light is indicated by white arrows. The orange arrow indicates the propagation direction of the reflected orange light, and the blue arrow indicates the reflected blue light. (*B*) Calculated far-field light-scattering pattern for different incidence angles (0–60°), showing three-directional reflections for near-normal incidence; the intensity of the central reflection decreases for increasing angle of incidence (compare Fig. 3 *B–D*). The slightly different color of the two side beams reflected at the thin-film cortex is due to natural variations of the barbule thickness (Fig. S5). (*C*) Diagrams illustrating the angle-dependent reflection of the breast feather barbule for increasing angles of incidence θ in the longitudinal symmetry plane.

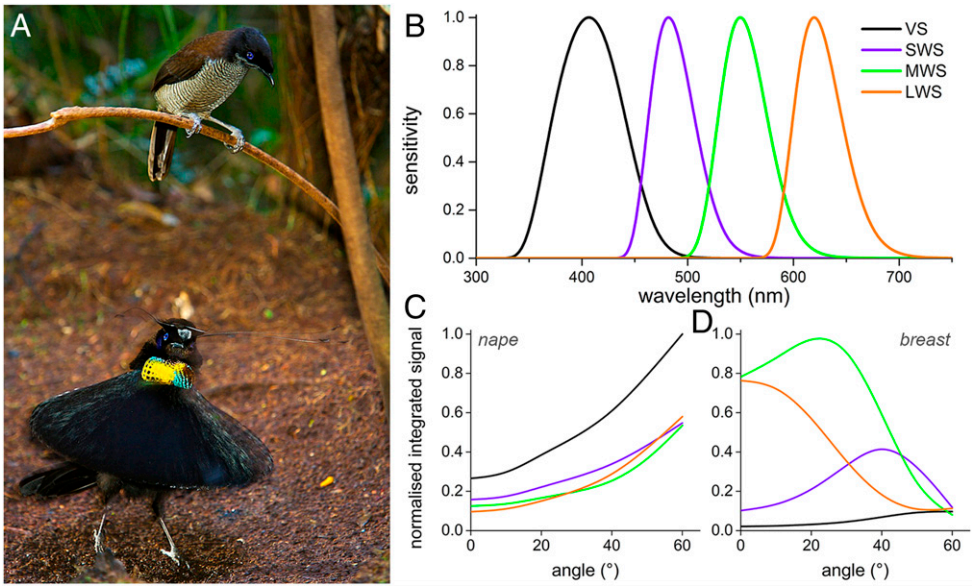

Fig. 5. Visibility in the dancing ritual and spectral tuning. (*A*) A female Western parotia, a close relative of Lawes' parotia, observing from an elevated position the ballerina dance of a possibly interesting male (photo courtesy of Tim Laman). (*B*) Spectral sensitivities of the four photoreceptors of the pigeon peaking in the violet, blue, green, and red, respectively (after ref. 25). (*C* and *D*) Normalized integrated signals in each photoreceptor channel for the angle-dependent spectra of the occipital (*C*) and breast (*D*) feather, calculated by multiplying the barbule reflectance spectra (Figs. 2 and 3) with the photoreceptor spectral sensitivities. Each feather type has a unique optical signature, particularly important in the dancing ritual of the male bird-of-paradise (see *Biological Implications and Connection to Bird Vision* for details).

(medium-wavelength–sensitive), and 620 nm (long-wavelength–sensitive) (Fig. 5*B* and refs. 24, 25). Convolving the spectral sensitivities with the reflectance spectra measured at various angles (Fig. 5 *C* and *D*) shows that the occipital feathers depend similarly on the angle of illumination but activate all spectral photoreceptors at the same time. The breast feathers, however, rather selectively activate certain photoreceptors depending on the angle of light incidence. This suggests that the relative excitation of the different photoreceptors by the broad-band reflecting occipital feathers remains rather constant during the spatially changing, rotating pattern, whereas the colorful breast feathers stimulate the different receptors of the tetrachromatic visual system in a temporally rapidly changing fashion. The black framing, due to strongly melanized feathers, will further facilitate a high optical contrast and increased visibility, to provide each feather with a unique optical signature.

Discussion

Structural coloration is widespread in nature and can be observed in butterflies (10, 26), beetles (27–30), fruits (31, 32), as well as fish (33, 34). Obviously, the control of the color of the reflected light as well as of the directional distribution is likely to be a behaviorally linked, key characteristic of many iridescent animals (35, 36).

As in many other birds (8, 9), the barbules of the feathers of the male Lawes' parotia are colored due to alternating layers of melanin rodlets and keratin (Fig. 1). The two investigated feather types are excellent examples of how slight alteration of the barbule morphology can strongly affect the reflection properties of the feathers: whereas the exceptionally ordered structure of the flat occipital feather barbules gives rise to a unidirectional silvery appearance, the boomerang-shaped breast feather barbules with the three angled mirrors produce a three-directional reflection.

Our analysis of the feather reflectance suggests that the mating displays of Lawes' parotia have the potential to be tuned to the spectral properties of the observing females' visual system (Fig. 5), especially because the spectral properties of avian photoreceptors only marginally vary over different genera (23, 24). So far there have been no direct tests of how birds respond to complex optical effects that are produced by structural colors, as those of the strongly saturated and highly dynamic reflections created by the parotia feathers. The type of specialized movements together with the tuning to vision however strongly indicates a positive correlation (36). Interestingly, most male birds-of-paradise (Paradisaeidae) have sparkling and extraordinary displays, like the strongly shape-shifting Superb Bird of Paradise, *Lophorina superba*, or the highly iridescent Magnificent Riflebird, *Ptiloris magnificus* (see, e.g., www.birdsofparadiseproject.org/ or refs. 1, 2). A comparative investigation of the highly specialized feathers and the visual system will elucidate the evolution of avian plumage as well as the importance of key variations in barbule morphology (37) and feather color in connection to the visual ecology of avian photoreceptors (23, 24).

From an optics perspective, the detailed quantification of the angle-dependent light reflection, often characterized as the bi-directional reflectance distribution function (see refs. 17, 38), will provide a more complete understanding of the mechanisms that underlie the performance of the photonic designs of complex samples. FDTD modeling, as a fully vectorial 3D Maxwell solving technique, proves to be an extremely powerful computational method that is very general with few inherent approximations to the Maxwell equations. By implementation of arbitrary geometries and correct material parameters, FDTD modeling thus allows one to gain deep insight into the light–matter interactions underlying the optical response of complex biophotonic structures. The reflectance spectra calculated for both the occipital and breast feather barbules are in striking agreement with the experimentally measured reflectance properties (Figs. 2 and 3), thus showing the validity, but also the predictive power, of the FDTD approach. FDTD therefore clearly is the method of choice for quantitative understanding of the optics of biophotonic structures.

Methods

Feather Samples. *P. lawesii* feathers were from specimens in the Queensland Museum and the Natural History Museum Naturalis. N. J. Marshall (University of Queensland, Brisbane, Australia) provided photographs of the bird

plumage (Fig. 1 *B* and *C*); T. Laman (Tim Laman Photography, Lexington, MA) provided habitat photographs (Figs. 1*A* and 5*A*).

Anatomy. The internal structure of the barbules was investigated by TEM, using a Hitachi 7100 transmission electron microscope. A piece of a feather was embedded in a mixture of Epon and Araldite following standard procedures (19).

Spectrophotometry. Angle- and polarization-dependent reflectance spectra of the feathers were acquired with an angle-resolved reflectance measurement setup (for more detail on the setup see ref. 19) based on a pair of optical fibers that could be rotated independently around the same axis, one acting as the light source, the other as the light collector, connected to an AvaSpec-2048–2 spectrometer (Avantes). The feathers were placed with the barbules perpendicular to the rotation axis, and the light reflectance spectra were measured as a function of the angle of light incidence and the polarization state. To measure the iridescence, both fibers were rotated in opposite, equally spaced steps of 10° from the center of the barbule. The light source was a xenon lamp. For all reflectance measurements, a white diffuse reflectance tile (Avantes WS-2) served as a reference.

Imaging Scatterometry. We examined the far-field, 180° hemispherical angular distribution of the light scattered by single barbules using an imaging scatterometer built around an ellipsoidal mirror (17, 19). We applied narrow-aperture (~5°) as well as wide-aperture (180°) illuminations supplied by xenon lamps. A piece of MgO served as a white reference.

FDTD Modeling. The light scattering by the internal structure of the barbs was simulated with the 3D FDTD method for different cross-sections of occipital as well as breast feather barbules obtained from TEM images. For the simulations we used TDME3D, a massively parallel Maxwell equation solver (15, 28). The TEMs were grayscaled and to each respective grayscale refractive index values, derived from Jamin–Lebedeff interference microscopy (Fig. S1 and refs. 13, 39), were assigned. The simulations were performed on the IBM BlueGene/P of the University of Groningen. One simulation run, which is the calculation for one structure, one wavelength, one polarization state, and one incidence angle, required a memory of approximately 150 GB.

ACKNOWLEDGMENTS. We thank Prof. Ulli Steiner and two anonymous reviewers for constructive comments, Hein Leertouwer for ongoing collaboration, Aidan Vey for proofreading, Dr. Julian Thorpe for the electron micrographs, and Prof. Justin Marshall and Dr. Tim Laman for providing photographs. This study was financially supported by the Air Force Office of Scientific Research/European Office of Aerospace Research and Development (Grant FA8655-08-1-3012 to D.G.S.) and the National Computing Facilities Foundation, The Netherlands.

1. Frith CB, Beehler BM (1998) *The Birds of Paradise* (Oxford University Press, Oxford).
2. Laman T, Scholes E (2012) *Birds of Paradise: Revealing the World's Most Extraordinary Birds* (National Geographic, Washington, DC).
3. Scholes E (2008) Structure and composition of the courtship phenotype in the bird of paradise Parotia lawesii (Aves: Paradisaeidae). *Zoology (Jena)* 111(4):260–278.
4. Pruett-Jones SG, Pruett-Jones MA (1990) Sexual selection through female choice in Lawes' parotia, a lek-mating bird of paradise. *Evolution* 44(3):486–501.
5. Stavenga DG, Wilts BD (2014) Oil droplets of bird eyes: Microlenses acting as spectral filters. *Philos Trans R Soc Lond B Biol Sci* 369(1636):20130041.
6. McGraw KJ (2006) Mechanics of melanin-based coloration. *Bird Coloration, Vol. I, Mechanisms and Measurements*, eds Hill GE, McGraw KJ (Harvard Univ Press, Cambridge, MA), pp 177–242.
7. Li Q, et al. (2012) Reconstruction of Microraptor and the evolution of iridescent plumage. *Science* 335(6073):1215–1219.
8. Durrer H (1977) Schillerfarben der Vogelfeder als Evolutionsproblem. *Denkschri Schweiz Nat Ges* 91:1–126.
9. Zi J, et al. (2003) Coloration strategies in peacock feathers. *Proc Natl Acad Sci USA* 100(22):12576–12578.
10. Kinoshita S (2008) *Structural Colors in the Realm of Nature* (World Scientific, Singapore).
11. Prum RO (2006) Anatomy, physics, and evolution of avian structural colors. *Bird Coloration, Vol. I, Mechanisms and Measurements*, eds. Hill G.E., McGraw K.J. (Harvard Univ Press, Cambridge, MA), pp 295–353.
12. Stavenga DG, Leertouwer HL, Marshall NJ, Osorio DC (2011) Dramatic colour changes in a bird of paradise caused by uniquely structured breast feather barbules. *Proc Biol Sci* 278(1715):2098–2104.
13. Wilts BD (2013) Brilliant biophotonics: Physical properties, pigmentary tuning and biological implications. PhD Thesis (University of Groningen, Groningen, The Netherlands).
14. Taflove A, Hagness SC (2005) *Computational Electrodynamics: The Finite-Difference Time-Domain Method* (Artech House, Boston).
15. Michielsen K, De Raedt H, Stavenga DG (2010) Reflectivity of the gyroid biophotonic crystals in the ventral wing scales of the Green Hairstreak butterfly, *Callophrys rubi*. *J R Soc Interface* 7(46):765–771.
16. Yee K (1966) Numerical solution of initial boundary value problems involving Maxwell's equations in isotropic media. *IEEE Trans Antenn Propag* 14:302–307.
17. Stavenga DG, Leertouwer HL, Pirih P, Wehling MF (2009) Imaging scatterometry of butterfly wing scales. *Opt Express* 17(1):193–202.
18. Wilts BD, Michielsen K, De Raedt H, Stavenga DG (2012) Hemispherical Brillouin zone imaging of a diamond-type biological photonic crystal. *J R Soc Interface* 9(72): 1609–1614.
19. Stavenga DG, Wilts BD, Leertouwer HL, Hariyama T (2011) Polarized iridescence of the multilayered elytra of the Japanese jewel beetle, *Chrysochroa fulgidissima*. *Philos Trans R Soc Lond B Biol Sci* 366(1565):709–723.
20. Born M, Wolf E (1975) *Principles of Optics* (Pergamon, Oxford).
21. Leertouwer HL, Wilts BD, Stavenga DG (2011) Refractive index and dispersion of butterfly chitin and bird keratin measured by polarizing interference microscopy. *Opt Express* 19(24):24061–24066.
22. Scholes E (2008) Evolution of the courtship phenotype in the bird of paradise genus Parotia (Aves: Paradisaeidae): Homology, phylogeny, and modularity. *Biol J Linn Soc Lond* 94(3):491–504.
23. Ödeen A, Håstad O, Alström P (2011) Evolution of ultraviolet vision in the largest avian radiation - the passerines. *BMC Evol Biol* 11:313.
24. Hart NS (2001) The visual ecology of avian photoreceptors. *Prog Retin Eye Res* 20(5): 675–703.
25. Hart NS, Vorobyev M (2005) Modelling oil droplet absorption spectra and spectral sensitivities of bird cone photoreceptors. *J Comp Physiol A Neuroethol Sens Neural Behav Physiol* 191(4):381–392.
26. Srinivasarao M (1999) Nano-optics in the biological world: Beetles, butterflies, birds, and moths. *Chem Rev* 99(7):1935–1962.
27. Galusha JW, Richey LR, Gardner JS, Cha JN, Bartl MH (2008) Discovery of a diamond-based photonic crystal structure in beetle scales. *Phys Rev E Stat Nonlin Soft Matter Phys* 77(5 Pt 1):050904.
28. Wilts BD, Michielsen K, Kuipers J, De Raedt H, Stavenga DG (2012) Brilliant camouflage: Photonic crystals in the diamond weevil, *Entimus imperialis*. *Proc Biol Sci* 279(1738):2524–2530.
29. Seago AE, Brady P, Vigneron J-P, Schultz TD (2009) Gold bugs and beyond: A review of iridescence and structural colour mechanisms in beetles (Coleoptera). *J R Soc Interface* 6(Suppl 2):S165–S184.
30. Vukusic P, Hallam B, Noyes J (2007) Brilliant whiteness in ultrathin beetle scales. *Science* 315(5810):348.
31. Vignolini S, et al. (2012) Pointillist structural color in *Pollia* fruit. *Proc Natl Acad Sci USA* 109(39):15712–15715.
32. Roberts NW, Marshall NJ, Cronin TW (2012) High levels of reflectivity and pointillist structural color in fish, cephalopods, and beetles. *Proc Natl Acad Sci USA* 109(50): E3387, author reply E3388.
33. Jordan TM, Partridge JC, Roberts NW (2012) Non-polarizing broadband multilayer reflectors in fish. *Nat Photonics* 6(11):759–763.
34. Mäthger LM, Denton EJ, Marshall NJ, Hanlon RT (2009) Mechanisms and behavioural functions of structural coloration in cephalopods. *J R Soc Interface* 6(Suppl 2): S149–S163.
35. Vukusic P (2011) Structural colour: Elusive iridescence strategies brought to light. *Curr Biol* 21(5):R187–R189.
36. Doucet SM, Meadows MG (2009) Iridescence: A functional perspective. *J R Soc Interface* 6(Suppl 2):S115–S132.
37. Maia R, Rubenstein DR, Shawkey MD (2013) Key ornamental innovations facilitate diversification in an avian radiation. *Proc Natl Acad Sci USA* 110(26):10687–10692.
38. Vukusic P, Stavenga DG (2009) Physical methods for investigating structural colours in biological systems. *J R Soc Interface* 6(Suppl 2):S133–S148.
39. Stavenga DG, Leertouwer HL, Wilts BD (2013) Quantifying the refractive index dispersion of a pigmented biological tissue using Jamin-Lebedeff interference microscopy. *Light Sci Appl* 2:e100.